Dear editor and referee#1,

Thank you very much for your time and attentions on this work. The comments and suggestions are very useful to improve our manuscript. Following is a point-by-point response to referee #1's comments. Texts in black are the comments, those in blue are our responses. All the line numbers mentioned in responses are referred to the manuscript with changes marked.

We hope that you will find the changes satisfactory and we are looking forward to hearing from you soon.

---

(1) In model validation (section 3.1), the authors compare the simulated $J[NO_2]$ with the observations. In addition to $J[NO_2]$, $J[O_3{}^1D]$ is also important in affecting the ozone photochemical production. Comparison on $J[O_3{}^1D]$ will show more sufficient evidence to demonstrating the well model performance in simulating photolysis rates. If the authors have the observations of $J[O_3{}^1D]$, please add the comparison of $J[O_3{}^1D]$.

Reply: Thank you for this comment. $J[O_3{}^1D]$ is indeed important in ozone photochemistry. Comparison on $J[O_3{}^1D]$ is important and necessary in photolysis rates validation. However, we didn't have the data before. Fortunately, we now have gathered the observations of $J[O_3{}^1D]$ at Xianghe station, and added the comparison of $J[O_3{}^1D]$ in the revised manuscript. Like the comparison of $J[NO_2]$, both the time series of $J[O_3{}^1D]$ and the relevant model performance metrics showed a good agreement between the observations and simulations. The model validations on $J[NO_2]$ and $J[O_3{}^1D]$ suggested that the WRF-Chem model performed very well in simulating the photolysis rates. Details can be checked in the revised manuscript in section 3.1.2.

(2) The authors showed that $J[NO_2]$ was enhanced at altitude above 1.3 km which is due to the enhancement of the light caused by the light-scattering effect of aerosols.

Discussions on the compositions of the aerosols and their effects on $J[NO_2]$ over this place are necessary. Please add them in the manuscript.

Reply: Thank you for your comment. Based on the optical properties of aerosols, they can be classified into light-scattering aerosols and light-absorbing aerosols. Before talking about the comprehensive effects of aerosols on $J[NO_2]$, it's necessary to present the effects of light-scattering aerosols and light-absorbing aerosols on $J[NO_2]$, respectively.

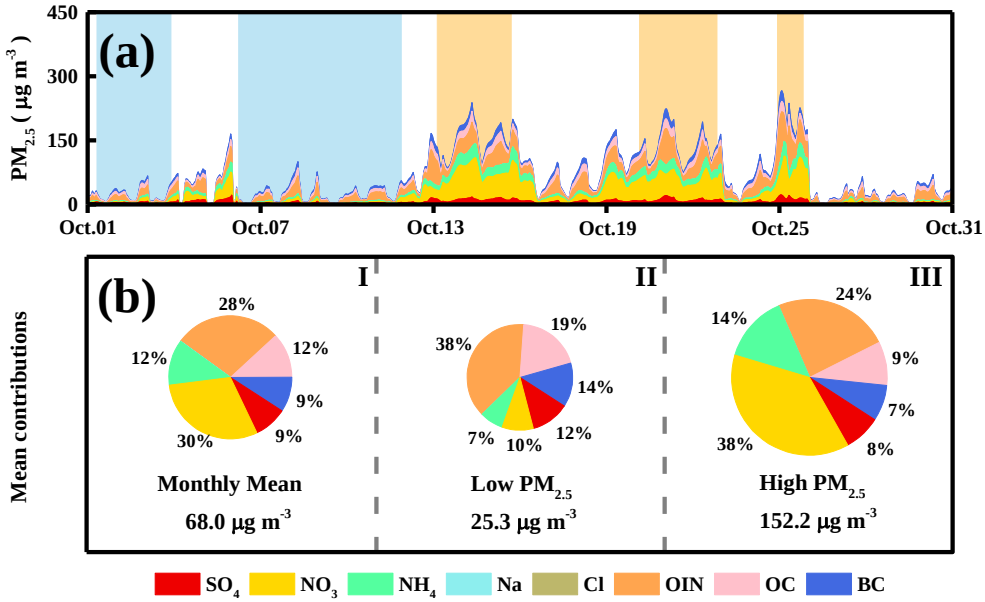

Figure R1. Time series (a) and mean contributions (b) of the simulated aerosol species at Xianghe station during Oct. 2018. I for the whole month; II for clean days (blue shaded parts in a); III for polluted days (yellow shaded parts in a).

In this study, MOSAIC-8bins was used as the aerosol chemistry mechanism. This mechanism includes eight aerosols species: Sulfate (SO_4), Nitrate (NO_3), Ammonium (NH_4), Sodium (Na), Chlorine (Cl), Organic Carbon (OC), Black Carbon (BC), and, Other Inorganics (OIN). Based on Fig. 2c in manuscript, concentrations of all the simulated aerosols species and their relative contributions to the total concentration of $PM_{2.5}$ at Xianghe station are shown in Fig. R1. During Oct. 2018, the mean concentration of $PM_{2.5}$ was 68.0 μg m^{-3} at Xianghe station. Among all the species, NO_3 and OIN contributed significantly which accounted for 30% and 28% to the total

concentration of $PM_{2.5}$; SO_4, NH_4, BC, and OC accounted for ~10%, respectively; Na and Cl showed few contributions during Oct. 2018. Under the "clean" condition (blue shaded parts in Fig. R1a and the pie chart II in Fig. R1b), the mean concentration of $PM_{2.5}$ decreased to 25.3 μg m^{-3} and OIN contributed (accounted for 38%) more than NO_3 did (accounted for 10%). On the contrary, OIN contributed (accounted for 24%) less than NO_3 did (accounted for 38%) when it was under the "polluted" condition (yellow shaded parts in Fig. R1a and the pie chart III in Fig. R1b).

Table R1. Refractive indexes of the aerosol species at each wave band in WRF-Chem model

wave band	300nm		400nm		600nm		999nm	
refr. index[a] / species	real[b]	imaginary[c]	real	imaginary	real	imaginary	real	imaginary
SO4	1.52	1.00×10^{-9}	1.52	1.00×10^{-9}	1.52	1.00×10^{-9}	1.52	1.75×10^{-9}
NO3	1.50	0.00	1.50	0.00	1.50	0.00	1.50	0.00
NH4	1.50	0.00	1.50	0.00	1.50	0.00	1.50	0.00
Na	1.51	8.66×10^{-7}	1.50	7.02×10^{-8}	1.50	1.18×10^{-8}	1.47	1.50×10^{-4}
Cl	1.51	8.66×10^{-7}	1.50	7.02×10^{-8}	1.50	1.18×10^{-8}	1.47	1.50×10^{-4}
OC	1.45	0.00	1.45	0.00	1.45	0.00	1.45	0.00
BC	1.85	0.71	1.85	0.71	1.85	0.71	1.85	0.71
OIN	1.55	3.00×10^{-3}	1.55	3.00×10^{-3}	1.55	3.00×10^{-3}	1.55	3.00×10^{-3}

[a] refr. index = refractive index; [b] real = real part; [c] imaginary = imaginary part

According to the source code of WRF-Chem model, the refractive index of each species was listed in Table R1. BC is a typical light-absorbing aerosol (Bond et al., 2004; 2013). Second to BC, OIN is also treated as light-absorbing aerosol since the imaginary part of which being larger than that of other species. The remaining species are treated as light-scattering aerosols. In order to showing the effects of the two types of aerosols on $J[NO_2]$, two more parallel experiments (Exp3 and Exp4) were designed: Exp3,

photolysis rate calculation without considering the optical properties of light-scattering aerosols; Exp4, photolysis rate calculation without considering the optical properties of light-absorbing aerosols. By comparing the results of Exp3 and Exp4 with the results of Exp1 respectively, the effects of light-absorbing aerosols and light-scattering aerosols on $J[NO_2]$ profile can be figured out.

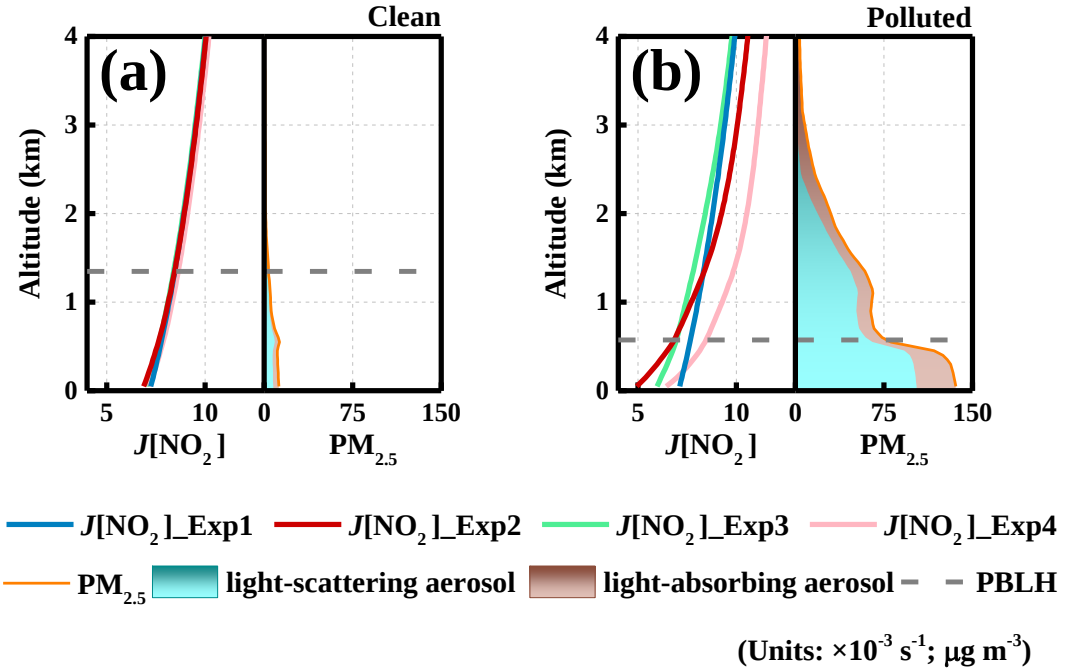

Figure R2. Mean profiles of $J[NO_2]$ and types of aerosols with diameter equal or less than 2.5 μg at 12:00 in clean days (a) and polluted days (b). Mean PBL height of the two kinds of days are also presented in (a) and (b), respectively.

Same as the data collection rule of Fig.3 in the manuscript but for the four experiments, the $J[NO_2]$ profiles under the low-level aerosol condition (clean) and high-level aerosol condition (polluted) at noon (12:00) are presented in Fig. R2. Correspondingly, the profiles of the two types of aerosols (cyan and brown shades) under clean and polluted conditions are also presented in Fig. R2a and R2b, respectively. Under clean condition (Fig. R2a), aerosols were at very low levels and didn't impact $J[NO_2]$ significantly. Consequently, the four profiles didn't show significant differences in vertical direction. Under polluted condition (Fig. R2b), the concentrations of $PM_{2.5}$

were at relatively high levels in the lowest 1.3 km ($PM_{2.5}$ with mean concentration of 90.0 μg m^{-3}; light-absorbing aerosols and light-scattering aerosols are 19.4 μg m^{-3} and 70.6 μg m^{-3}, respectively), especially in the PBL, where the mean concentration of $PM_{2.5}$ reached 123.1 μg m^{-3} (light-absorbing aerosols and light-scattering aerosols are 28.4 μg m^{-3} and 94.7 μg m^{-3}, respectively). Since light-absorbing effect of light-absorbing aerosols, the incident solar irradiance was attenuated (Ding et al., 2016; Gao et al., 2018) and $J[NO_2]$ profile ($J[NO_2]$_Exp3) decreased along with the vertical direction. For light-scattering aerosols, since high concentration being located in lower layer, the incident solar radiation could be scattered backward and enhance the shortwave radiation in higher layer. In this case, $J[NO_2]$ ($J[NO_2]$_Exp4) aloft was enhanced. However, the incident solar irradiance was attenuated at the layers near the surface which leading to the decrease in $J[NO_2]$ near the surface. Combining the effects of the two types of aerosols, the light extinction of aerosols on $J[NO_2]$ ($J[NO_2]$_Exp2) decreased at the lowest 1.3 km but enhanced above 1.3 km.

Unfortunately, since lacking of relevant observations of the aerosol species, concentrations of the simulated aerosols species could not be validated and this may cause uncertainties to the impacts of different types of aerosols on $J[NO_2]$ profiles. Thus, we just present these results and discussions in the response material. However, our validations on $PM_{2.5}$, $J[NO_2]$, and $J[O_3{}^1D]$ are acceptable which suggested that the results on the light extinction of aerosols on photolysis rates and its effect on ozone concentrations which we discussed in our study are meaningful. In addition, our results are consistent with results from other study (Dickerson et al., 1997) which also demonstrate the validity of the results we presented in the manuscript.

It should be noted that different contributions of aerosol species could impact photolysis rates differently. Aerosols species contributed very differently at different places. Figuring out the effects of aerosols on $J[NO_2]$ profiles over East China is an interesting topic which being worthy of further studying.

(3) Line 99, add a comma after “combustion”

Reply: Thanks, we have added a comma after “combustion”. Please check the detail in

the revised manuscript at line 101.

(4) Line 135, add a comma after “episodes”

Reply: Thanks, we have added a comma after “episodes”. Please check the detail in the revised manuscript at line 138.

(5) Variables in Table 2 need to be added with units.

Reply: Thank you very much. Units of all the variables in Table 2 have been added. Details could be checked in the Table 2 in the revised manuscript.

(6) Caption of figure 6 needs to be updated. “CASE1” and “CASE2” should be replaced by “Exp1” and “Exp2”.

Reply: Thank you for the comment. We have updated the caption of figure 6. “CASE1” and “CASE2” have been replace by “Exp1” and “Exp2”. Please check the new caption of figure 6 in the revised manuscript.

Reference

Bond, T. C., Streets, D. G., Yarber, K. F., Nelson, S. M., Woo, J. H., and Klimont, Z.: A technology-based global inventory of black and organic carbon emissions from combustion, J. Geophys. Res., 109, D14203, https://doi.org/doi:10.1029/2003JD003697, 2004.

Bond, T. C., Doherty, S. J., Fahey, D. W., Forster, P. M., Berntsen, T., DeAngelo, B. J., Flanner, M. G., Ghan, S., Karcher, B., Koch, D., Kinne, S., Kondo, Y., Quinn, P. K., Sarofim, M. C., Schultz, M. G., Schulz, M., Venkataraman, C., Zhang, H., Zhang, S., Bellouin, N., Guttikunda, S. K., Hopke, P. K., Jacobson, M. Z., Kaiser, J. W., Klimont, Z., Lohmann, U., Schwarz, J. P., Shindell, D., Storlvmo, T., Warren, S. G., and Zender, C. S.: Bounding the role of black carbon in the climate system: A scientific assessment, J. Geophys. Res.: Atmos., 118, 5380–5552, https://doi.org/doi:10.1002/jgrd.50171, 2013.

Ding, A. J., Huang, X., Nie, W., Sun, J. N., Kerminen, V. M., Petaja, T., Su, H., Cheng, Y. F., Yang, X. Q., Wang, M. H., Chi, X. G., Wang, J. P., Virkkula, A., Guo, W. D., Yuan, J., Wang, S. Y., Zhang, R. J., Wu, Y. F., Song, Y., Zhu, T., Zilitinkevich, S., Kulmala, M., and Fu, C. B.: Enhanced haze pollution by black carbon in megacities in China, Geophys. Res. Lett., 43, 2873-2879, https://doi.org/10.1002/2016GL067745, 2016.

Dickerson, R. R., Kondragunta, S., Stenchikov, G., Civerolo, K. L., Doddridge, B. G., and Holben, B. N.: The impact of aerosols on solar ultraviolet radiation and photochemical smog, Science, 278, 827-830, https://doi.org/10.1126/science.278.5339.827, 1997.

Gao, J. H., Zhu, B., Xiao, H., Kang, H. Q., Pan, C., Wang, D. D., and Wang, H. L.: Effects of black carbon and boundary layer interaction on surface ozone in Nanjing, China, Atmos. Chem. Phys., 18, 7081-7094, https://doi.org/10.5194/acp-18-7081-2018, 2018.